FUNCTIONAL NETWORKS OF ANATOMIC BRAIN REGIONS

Burak Velioglu[⋆] *Emre Aksan*[⋆] *Itir Onal*[⋆] *Orhan Firat*[⋆] *Mete Ozay*[†] *and Fatos T. Yarman Vural*[⋆]

[⋆]Department of Computer Engineering, Middle East Technical University, Ankara, Turkey
{*velioglu, emre.aksan, itir, orhan.firat, vural*}*@ceng.metu.edu.tr*
[†]School of Computer Science, University of Birmingham, Birmingham, UK
m.ozay@cs.bham.ac.uk

Keywords fMRI, Functional Brain Network, MVPA,

ABSTRACT

In this study, we propose a new approach to construct a two-level functional brain network. The nodes of the first-level network are the voxels of the functional Magnetic Resonance Images (fMRI) recorded during an object recognition task. The nodes of the network at the second-level are the anatomic regions of the brain. The arcs of the first level are estimated by a linear regression equation for the meshes formed around each voxel. Neighbors of each voxel are determined by using a functional similarity metric. The node degree distributions of the voxel-level functional brain network are then used to estimate the node attributes and arc weights between the nodes of anatomic regions at the second level. The region-level functional brain network is then used to analyze the relationship among the anatomic regions of the brain during a cognitive process. Our results indicate that, although the neighborhood is defined functionally, voxels tend to make connections within the anatomic regions. Therefore, it can be deduced that nearby voxels work coherently during the cognitive task compared to the voxels apart from each other.

I. INTRODUCTION

Recently, the great challenge for understanding the sophisticated functional and physiological structure of brain is accelerated by the aid of new imaging and computing techniques [1]–[3]. Due to its non-invasive nature and high spatial and acceptable temporal resolution, fMRI is used as the primary source by the researchers to analyze how the brain functions.

It is well-known that high voxel intensity values in fMRI represent the active regions of the brain. Various studies, such as [4]–[8], elaborated this fact to describe and to identify the anatomic regions of the brain related to a specific cognitive task by using vast range of image processing methods, such as Principal Component Analysis, Independent Component Analysis, Search Light or Generalized Linear Models to select the relevant voxels for that cognitive task. However, considering the massively interconnected structure of the brain, voxel intensity values fall too short to represent the functions and structures of anatomic regions. The natural small-world network topology [9] of the brain suggests to develop brain connectivity models and graph based techniques to understand its task specific behavior.

Several studies in neuroscience [10]–[13] model the brain as a network, in which nodes correspond to voxels and edges between the nodes represent the connectivities among the voxels. In their study Baldassano et al. [17] observe that, different sub-regions of brain have different topology of sub-connectivities among the voxels. In addition to the varying topology, Zalesky et al. [18] shows that the strength of connectivities of brain networks also differ in different regions. In the Zalesky's study, the connectivity differences within regions were analyzed, yet interactions among the anatomic brain regions under a cognitive task is not explored.

In this study, first-level brain network is constructed using the voxels of fMRI data recorded during an object recognition task as nodes. Neighbors of each voxel are determined by using a functional similarity metric, meaning that two voxels are connected if they have *functionally similar* time series [15]. Note that in this approach, depending on the functional similarity, two spatially adjacent voxels may be connected or unconnected. The arc weights of each mesh formed around a seed voxel are estimated by a linear regression model fitted to the voxel intensity values, as suggested by Ozay et al. [14]. These weights, called *Mesh Arc Descriptors (MAD),* are assumed to represent the strength of the relationships among the voxels and voxel groups which correspond to anatomic regions. The mesh size of each individual voxel (the number of functional neighbors of a voxel) is estimated by optimizing Akaike's Final Prediction Error using the residual error of the linear regression equation as suggested by [16], [22]. The optimal mesh size indicates the degree of connectivity of a voxel to its functional neighbors. By combining the functional meshes formed around all voxels, a voxel-level network, in which, the nodes represent the voxels and edges represent the relationship among voxels, is obtained.

The suggested first-level network is then used to investigate the activities and interactions among and within the anatomic regions. The interactions among the anatomic brain regions are modeled and quantified by the node degree distributions and distributions of the arc weights of the suggested brain network. In this study, we assume that high node degrees indicate strong relations among the voxels and voxel groups. Therefore, the node degree distributions within

Thanks to TUBITAK agency for funding with grant no:112E315.

and between the anatomic regions indicate the strength of the interactions among the voxels residing in same and different anatomic regions, respectively.

The suggested two-level functional brain network is constructed for the data set generated by Mitchell et al. [19]. Then, the node degree distributions within and between the anatomic regions are obtained. It is observed that the connections formed within anatomic regions are denser than connections formed between different regions. Hence, the voxels residing in the same region are more correlated and perform more similarly under a cognitive task than the ones residing in separate regions. Moreover cortical regions, which are known as the most sophisticated part of the brain, form denser between and within connections. These findings are substantially consistent with the neurological findings of anatomical regions of the human brain.

II. DATASET

The dataset, employed in this study is collected by Mitchell et al. [19]. There are noun labels and line drawings from 12 semantic categories, namely; animals, body parts, buildings, building parts, clothing, furniture, insects, kitchen items, tools, vegetables, vehicles and other man-made items. 5 exemplars from each category are shown within each run, therefore 60 concrete objects are used for each run, and entire set of stimuli was presented 6 times during whole experiment, in a different random order. In the dataset, voxels are labeled using Automated Anatomically Labeling (AAL) [21] which has 116 different regions in total.

Siemens Allegra 3.0T scanner is used to acquire functional images, using a gradient echo EPI pulse sequence with TR = 1000 ms, TE = 30 ms and a 60° angle. Seventeen 5-mm thick oblique-axial slices were imaged with a gap of 1-mm between slices. The acquisition matrix was 64 x 64 with 3.125 x 3.125 x 5-mm voxels.

III. FUNCTIONAL BRAIN NETWORK

Let us start by defining the first-level functional brain network. Consider a data set of voxels $D = \{v(t_i, \bar{s}_j)\ , r_k\}$, where each voxel $v(t_i, \bar{s}_j)$ is labeled by an anatomic region, r_k, $k = \{1, 2, \ldots, R\}$ and R represents the number of anatomic regions in the data set. t_i represent the sample at time instant $i = \{1, 2, \ldots, T\}$ and $\bar{s}_j$ represent the voxel coordinates, $j = \{1, 2, \ldots, M\}$. Note that $\bar{s}_j$ is a three dimensional vector which represents the x, y and z coordinates of a voxel. The second-level functional regional brain network is defined as $FBN = \{N, C\}$, where each node, n_k from the node set N represents an anatomic region and the arc $c_{k,l}$ from the arc set C represents the degree of connectivity between the nodes n_k and n_l. The labels of the anatomic brain regions are defined by AAL. The estimation of the node attributes n_k and the estimation of the arc weights $c_{k,l}$ will be described in the next subsections.

III-A. Forming Local Meshes Around Each Voxel

The initial step of constructing the first-level functional brain network is to define a star mesh around each voxel,

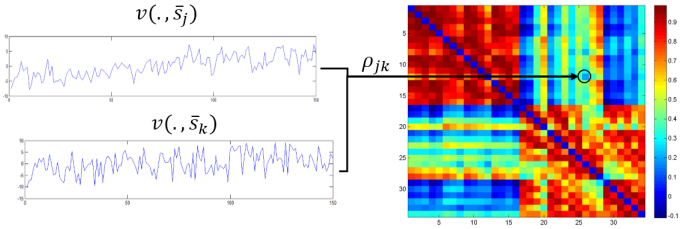

Fig. 1: A sample functional connectivity matrix formed by pairwise correlation measures. Each pairwise correlation measure ρ_{jk} is calculated between the time series of distinct voxels at location $\bar{s}_j$ and $\bar{s}_k$.

called seed voxel. The neighbors of the seed voxel is determined by a neighborhood system. In this study, the neighborhood system is based on the functional similarity of the time series between the voxel pairs, as suggested in [15]. Functional similarity is defined as the measure of *similarity* between time series of voxels. Therefore, the functional connectivity depends on the similarity measure. The *similarity* can be measured, for example, by estimating the correlation or covariance between pairs of time series. Therefore, the *p-nearest neighbors* of the seed voxel are selected based on the correlation among the voxels. In this approach *p-nearest neighbors* $\{v(t_i, \bar{s_k})\}_{k=1}^{p}$ of the seed voxel are the voxels whose zero-order correlations with the seed voxel are the maximum among the others. The zero-order correlation coefficient ρ_{jk} between two voxels at coordinates $\bar{s}_j$ and $\bar{s}_k$ is calculated by using the all time instances $\mathbf{t} = (t_1, t_2, ..., t_T)$,

$$\rho_{jk} = \frac{cov_{jk}\big(v(\mathbf{t}, \bar{s}_j),\ v(\mathbf{t}, \bar{s}_k)\big)}{\sqrt{var_j\big(v(\mathbf{t}, \bar{s}_j)\big) \cdot var_k\big(v(\mathbf{t}, \bar{s}_k)\big)}}, \qquad (1)$$

where cov_{jk} is the covariance of the signals measured at two voxels, and var_j is the variance of the signals measured at a voxel $v(\mathbf{t}, \bar{s}_j)$ and $\rho_{jk} \in [-1, 1]$.

The rationale behind using functional neighborhood is the well known phenomenon that the spatially close voxels are strongly coupled during cognitive processes [20]. Moreover, the assumption of spatially surrounding neighborhood in mesh arc descriptors for every voxel, may cause redundant meshes and arc weights for further analysis. A partial improvement to overcome this problem resides in functional neighborhood concept and the information comes from functional connectivity between distinct voxels. A sample functional connectivity matrix and pairwise correlation estimation is illustrated in Fig. 1

Motivated by the functionality regarding to cognitive processes, modeling relations between distinct regions or even voxels in the brain, brings vast opportunities for our studies. Functional connectivity is expected to capture patterns of deviations between distributed and often spatially remote regions in brain and constructed using an inter-regional analysis. In this study we employed functional connectivity in MAD by selecting functional neighbors for each voxel

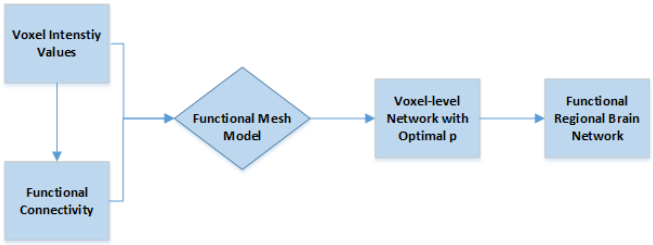

Fig. 2: Steps to obtain functional regional brain network

and constructing the meshes based on the functional neighborhood which results in a more discriminative information source.

III-B. Estimating the Mesh Arc Descriptiors

The arc weights of each local mesh, formed around a voxel, indicate the relationship between the *seed voxel* $v(t_i, \bar{s}_j)$ and its *p- functionally nearest neighbor* voxels $\{v(t_i, \bar{s_k})\}_{k=1}^{p}$, where t_i represent the sample at time instant $i = \{1, 2, \ldots, T\}$ and $\bar{s}_j$ represent the voxel coordinates $j = \{1, 2, \ldots, M\}$. The arc weights $a_{i,j,k}$ at the ith time sample between voxels located at $\bar{s}_j$ and $\bar{s}_k$ are called *Mesh Arc Descriptors (MAD)*.

In the mesh model, the relationship among a *seed voxel* $v(t_i, \bar{s}_j)$ and its neighboring voxels are defined as the linear combination between a seed voxel and its *p-nearest neighbor* voxels as follows;

$$v(t_i, \bar{s}_j) = \sum_{\bar{s}_k \in \eta_p} a_{i,j,k} v(t_i, \bar{s}_k) + \varepsilon_{i,j}(p), \qquad (2)$$

where $\varepsilon_{i,j}(p)$ is the error obtained during the estimation of the *MAD* features. *MAD* features are estimated using the Levinson - Durbin recursion [26] in which the variance of error $\varepsilon_{i,j}(p)$ of (2) is minimized.

A critical issue is to estimate the optimal mesh size p, which indicates the degree of connectivity of a node to its functional neighbors. The information theoretic method suggested for estimating the node degrees will be explained in subsection III-C.

III-C. Estimating the Optimal Mesh Sizes and Constructing the First-Level Functional Brain Network

The size of a mesh p defines the number of the neighboring voxels of a specified seed voxel in a functional mesh. As the mesh size increases, the seed voxel makes denser connections with an increased complexity whereas the model better fits the data with decreased error term $\varepsilon_{i,j}(p)$ of (2). Therefore, we [22] suggest to optimize the trade-off between the degree of fit, represented by the variance of error $\varepsilon_{i,j}(p)$ and the complexity, represented by the mesh size p by minimizing Akaike's Final Prediction Error (FPE) [23]. For each voxel at $\bar{s}_j$, we estimate an optimal mesh size $\hat{p}_j$, representing the optimal number of connectivities.

First, the squared error of (2) is calculated for each voxel and for each mesh size, as follows,

$$\varepsilon_{i,j}(p)^2 = \left(v(t_i, \bar{s}_j) - \sum_{\bar{s}_k \in \eta_p} a_{i,j,k} v(t_i, \bar{s}_k) \right)^2 . \qquad (3)$$

Then, the expected error for each voxel over all time samples is approximated by

$$\hat{E}_j = E_i(\varepsilon_{i,j}^2) \cong \frac{1}{T} \sum_{i=1}^{T} \varepsilon_{i,j}^2 , \qquad (4)$$

where $E_i(\cdot)$ is the expectation operator over the time instants t_i for a single voxel. Finally, we minimize Akaike's Final Prediction Error (FPE) in (5) with respect to the mesh size p so that we obtain the optimal mesh size for each voxel separately.

$$FPE_{j,\rho}(p) = \hat{E}_{j,\rho} \left(\frac{M + p + 1}{M - p - 1} \right) \qquad (5)$$

where M represents the number of voxels. $FPE_{j,\rho}(p)$ is calculated for mesh size in a pre-defined interval $[p_{min}, p_{max}]$. After that, the optimal mesh size for voxel at coordinates $\bar{s}_j$ is selected as the one that minimizes $FPE_j(p)$ using,

$$\hat{p}_j = \underset{p \in [p_{min}, p_{max}]}{\arg\min} \left(FPE_j(p) \right). \qquad (6)$$

In the above formulation, $\hat{p}_j$ represents the optimal mesh size for a voxel at coordinates $\bar{s}_j$, estimated using FPE and $[p_{min}, p_{max}]$ is an interval which is determined empirically.

The local functional meshes with optimal mesh sizes and mesh arc descriptors are concatenated to construct a first-level functional brain network. In this network, each voxel is connected to its functionally closest *p-nearest neighbors*, where the optimal value of p varies for each voxel, showing the degree of connectivity of a node. Although the network topology doesn't change through the cognitive task, the arc weights vary according to stimulus shown to subject. There are two directed arcs between each pair of nodes, where the arc weights are estimated by the linear regression model of equation 2.

The first-level functional brain network constructed in this study is too large to extract information about the interactions among the brain regions. There are approximately 20,000 nodes and 400,000,000 arc weights to evaluate the anatomical regions and their relations. Also, there are substantial amount of redundancies among the local meshes. Therefore, one needs to compress the information represented in the voxel-level network and reduce the redundancies among the local meshes.

There are many approaches in Graph Theory to reduce the number of nodes and arcs of a network [27], [28]. In this study, we suggest a simple method to modify the first-level functional brain network in order to obtain a second-order *functional regional brain network* which models the relationship among the anatomic regions. For this purpose, we define a new network topology, $FBN = \{N, C\}$, where each node, N_k represents an anatomic region and the arc $c_{k,l}$ from the set C represents the total number

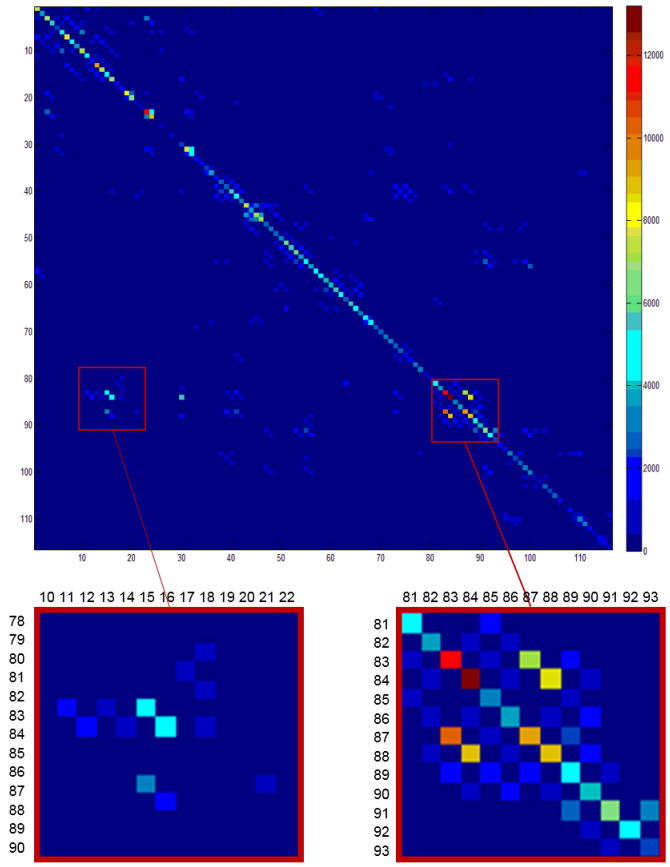

10	Right middle frontal gyrus, orbital part
11	Left opercular part of inferior frontal gyrus
12	Right opercular part of inferior frontal gyrus
13	Left area triangularis
14	Right area triangularis
15	Left orbital part of inferior frontal gyrus
16	Right orbital part of inferior frontal gyrus
17	Left rolandic operculum
18	Right rolandic operculum
19	Left supplementary motor area
20	Right supplementary motor area
21	Left olfactory cortex
22	Right olfactory cortex
78	Right thalamus
79	Left transverse temporal gyri
80	Right transverse temporal gyri
81	Left superior temporal gyrus
82	Right superior temporal gyrus
83	Left superior temporal pole
84	Right superior temporal pole
85	Left middle temporal gyrus
86	Right middle temporal gyrus
87	Left middle temporal pole
88	Right middle temporal pole
89	Left inferior temporal gyrus
90	Right inferior temporal gyrus
91	Left crus I of cerebellar hemisphere
92	Right crus I of cerebellar hemisphere
93	Left crus II of cerebellar hemisphere

Fig. 3: Interactions between AAL anatomical regions. Rows and columns from 1 to 116 represents AAL region ids. Regions in the left red square are the ones connected most densely with other regions and regions in the right red square are the ones connected most densely within itself.

of connections between the regions n_k and n_l. The total number of connections, $c_{k,l}$ are obtained from the first-level functional brain connectivity network, by simply counting the number of voxel connections between each anatomic region pair. The node attributes n_k, of the FBN are assigned by estimating the expected values of the node degrees in each anatomic region. The total number of connections $c_{k,l}$, formed between the voxels belonging to region r_k and r_l defines the edge weight between the nodes n_k and n_l corresponding to the regions r_k and r_l. Notice that, the connections formed within a single anatomic region are collapsed and are not shown in the second-level *functional regional brain network*.

III-D. Estimating the Node Degree Distributions of the Functional Regional Brain Network

After constructing the second-level *functional regional brain network* for a participant, we can separate the arcs $c_{k,l}$ of the FBN in two disjoint sets, as the within region and between region arc sets. If the arc connects two voxels belonging to the same region labeled with r_k, it's represented by $c_{k,k}$ and $c_{k,k} \in \check{C}_k$ where $\check{C}_k$ represents the set of all arcs within the region labeled with r_k. On the other hand, if an arc $c_{k,l}$ is formed between the voxels belonging to separate regions r_k and r_l, then $c_{k,l} \in \hat{C}_{kl}$ where $\hat{C}_{kl}$ denotes the connections made between the voxels belonging to region r_k and region r_l. Node degree distributions are estimated for all the within region $\check{C}_k$ and between region arc sets $\hat{C}_{kl}$.

The estimated $\hat{p}_j$ value defines the degree of connectivity at a specific location of the brain. With higher values of $\hat{p}_j$, we expect that the corresponding voxel make denser connections during the cognitive task. Similarly, activation in an anatomic brain region can be identified in terms of the total connectivity formed by the voxels located in that region. If $\check{C}_k$ dominates the sum of $\hat{C}_{kl}$ value, then we may conclude that the anatomic region r_k is highly connected within itself. In other words, the voxels belonging to the anatomic region labelled with r_k tend to make more connections with the voxels also in the same region r_k rather than the ones in other anatomic regions. On the other hand, the evidence of greater $\hat{C}_{kl}$ sum over all regions other than r_k reveals the fact that region r_k is highly correlated with other regions.

Fig. 2 represents the steps to obtain second-level *functional regional brain network*. As it can be seen, after functional mesh is formed around all voxels using a functional

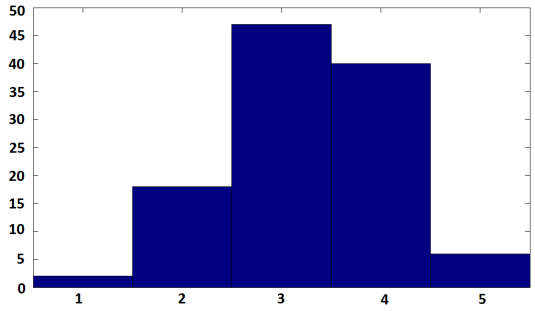

Fig. 4: Histogram of functional & spatial neighborhood match. For each anatomic region, sets of nearest 5 spatial and densest 5 functional neighbors are compared. Vertical axis represents number of regions and the horizontal axis represents the number of common elements in both sets. (Top 5 neighbors are selected since the minimum number of functional connections for a region is 5.)

neighborhood, they are used to form a first-level voxel-level network, where the number of edges among voxels are optimized using FPE. As a result, the *functional regional brain network* is formed by representing all of the voxels within a region as a single node and represents the total number of arcs between regions as the edges.

IV. EXPERIMENTS

In our experiments, we estimated the interactions between and within anatomic regions using the data set collected by Mitchell et al. [19]. Then, we constructed a functional mesh around each voxel using zero-order correlation as the distance metric. After that, the optimal mesh size representing the degree of connectivity is calculated for each voxel by minimizing Akaike's Final Prediction Error. We assumed that, the greater the number of neighbors, the more active the specified voxel during the cognitive task. From voxel-level interactions, we moved to region-level and explored the interactions of *functional regional brain network*. The total number of interactions between the anatomic regions, represented in *functional regional brain network* shows the strength of connectivity between the regions during the cognitive task. Moreover, the total number of interactions within region, observed in first-level brain network, reflects the degree of connectivity within the specified anatomic region.

Fig. 3 shows the degree of connectivities representing relations between regions. Note that, the diagonal of the matrix represents the within region connectivities whereas off diagonal entries represent the pairwise relationships among two distinct regions. The darker red colors in the diagonal of the matrix indicates that the regions are connected more densely within itself whereas darker blue is an indicator of sparse connectivities within regions. As it can be seen from Fig. 3, almost all regions are primarily connected to themselves. More precisely 46% of all edges are found as within region connections. Furthermore, % 91 of all anatomical regions are primarily connected to themselves, and the remaining ones are generally the ones including a small number of voxels.

Functional connectivity enables denoting relationships among spatially-distinct brain regions that correlate in a cognitive task [24], [25]. In other words, the voxels in an anatomic region tend to make connections with the voxels belonging to the same region. Notice that, since the neighborhood is defined functionally, a spatial constraint was not applied during the selection of *p-nearest neighbors*. However, we observed that the functionally nearest neighbors of a seed voxel are mainly the ones that reside in the same anatomical region with the seed voxel. Fig. 4 reflects the histogram of functional and spatial neighborhood match. For each anatomic region, we detected the 5 anatomic

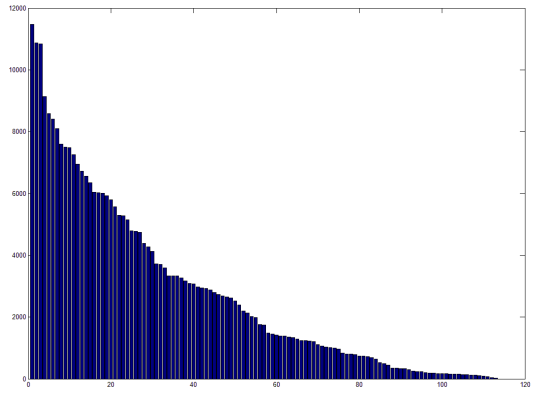

Fig. 5: Between connectivity degree of each node is plotted in sorted order. Each bar represents a region. Connectivity degree of a region is summation of all outgoing edges

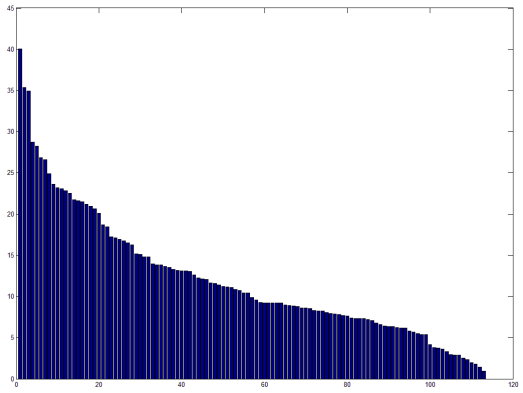

Fig. 6: Within node degrees are plotted in sorted order which calculated as $size(\tilde{C}_k)/size(r_k)$. Each bar represents a region.

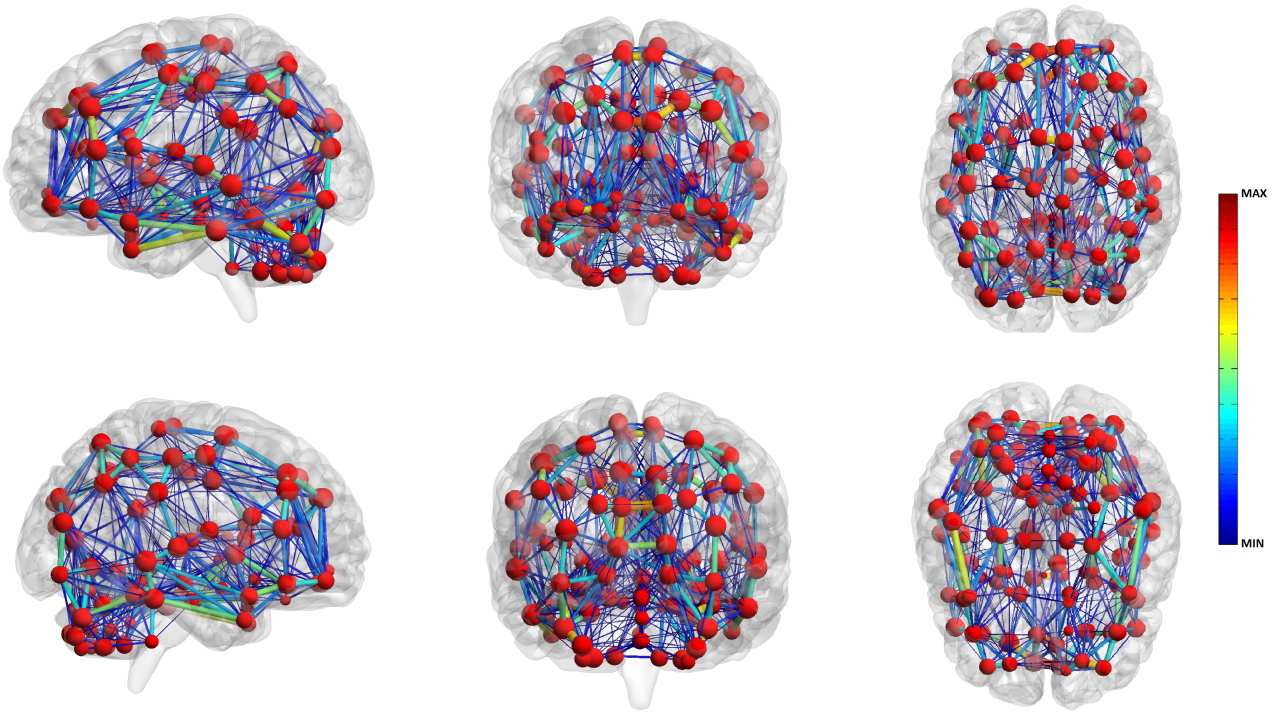

Fig. 7: Illustration of functional regional brain networks from sagittal, axial and coronal views. Spheres are center points of regions and edges are interactions between them. Thicker and red edges demonstrate denser connection between corresponding regions, whereas thinner and blue edges demonstrate sparse connection. Radius of spheres represents size of the anatomical region in terms of voxel numbers. Edge weight between two regions r_k and r_l is calculated as division of $c_{k,l}$ with total number of voxels in both regions r_k and r_l. [29]

regions which make the densest functional connections with the specified region and we explored whether they are also the spatially closest regions to that specified region. From Fig. 4 it can be seen that, among 5 regions which make the densest connection with a specified region, generally 3 or 4 of them are also the in the top 5 spatially closest regions list. In other words, regions that are functionally connected are usually spatially close to each other.

Within and between connectivity degree vary by region. Right superior temporal pole, left superior temporal pole, left superior frontal gyrus - medial part, left area triangularis, left middle temporal pole, right middle temporal pole, right superior frontal gyrus - medial part, left supplementary motor area, left anterior cingulate gyrus, left middle frontal gyrus - lateral part are the regions have the densest connectivity within themselves, respectively. Whereas right superior temporal pole, left crus I of cerebellar hemisphere, left superior frontal gyrus - medial part, left superior temporal pole, left superior frontal gyrus - dorsolateral, left fusiform gyrus, right superior frontal gyrus - medial part, left calcarine sulcus, left middle frontal gyrus - lateral part, left middle temporal pole are the regions have the densest connectivity with other regions. Fig. 5 and Fig. 6 demonstrates the varying within and between connectivity degrees, respectively.

We also observed that an anatomic region makes dense functional connections with a few other regions and it either forms sparse connections or does not form any connection with the remaining regions. In other words, among distinct regions either sparse or no connections are formed. Therefore, our *functional regional brain network* also includes a small-network topology in which a node is connected to a few neighboring nodes.

Active functional connectivity patterns in Fig. 7 are also substantially consistent with anatomical findings. A pathway existing from optic nerves (partially) to brain stem to occipital lobe shows us that the participant is presented something and both reflex and central vision system is aware of that. Dense interaction within occipital lobe demonstrate that participant understands what is shown to him since that part of the brain is mostly active when a person tries to understand what he observes. In our model, within the frontal lobe denser but weaker activities are formed, which is consistent with the finding that frontal lobe of the brain is responsible for high level functions and requires denser connections. Furthermore, the dense connections within the limbic system shows that the participant's memory related

to presented objects are activated. Tight interaction between region 83 and 87 demonstrates collaborative work of smell and vision takes great role within object recognition task. Furthermore, connectivity between region 15, which resides in the Broca's area, and 83 shows the interaction between remembering the name of object and visual stimulus.

V. CONCLUSION

In this study, we proposed a region-level brain network, called *functional regional brain network*, constructed by converting voxel-level connectivities into connectivities among regions. Our purpose was to explore how the pre-defined anatomic regions of the brain interact during a cognitive task. While anatomic regions represent nodes of this network, aggregation of connectivity patterns of voxels located within the anatomic regions defines the edges.

We observed that, voxels are inclined to make connections within their regions rather than with the ones from other regions. In other words, connections within region are much more than the connections between region. Furthermore, we explored that the regions make the densest connections with the spatially closest ones. Therefore, we concluded that, functionally similar voxels are also the ones which are spatially closer to each other. From *functional regional brain network*, we observed that a region makes dense connections with a few of its spatially nearest neighbors and makes sparse or no connections with the remaining regions. Our finding is consistent with the small-network topology of brain.

In this study, we only employed the node degree distributions of regions to represent a functional brain network. Notice that, we obtained a single topology for all cognitive states where the edges correspond to the number of interactions among regions. However, although they share the same optimal mesh size, different classes have different *MAD* values among voxels. Therefore, as a future work, we will also analyze how the distributions of arc weights (*MAD*) vary among anatomic regions. Moreover, since the network topology is same for all classes while the *MAD* values vary, they can be used as features to classify various cognitive states.

VI. ACKNOWLEDGEMENTS

We thank Gulsah Sahan for invaluable explanations about the anatomy of the brain. This project is supported by TUBITAK Project, 112E315. Mete Ozay was supported by the European commission project PaCMan EU FP7-ICT, 600918.

VII. REFERENCES

[1] B. Chai, D. B. Walther, D. M. Beck, and F.-F. L., Exploring Functional Connectivity of the Human Brain using Multivariate Information Analysis, Advances in neural information processing systems, pp. 1-9, 2009

[2] K. A. Norman, S. M. Polyn, G. J. Detre, and J. V. Haxby, Beyond mind-reading: multi-voxel pattern analysis of fMRI data., Trends in cognitive sciences, vol. 10, no. 9, pp. 424-30, Sep. 2006.

[3] X. Wang, R. Hutchinson, and T. M. Mitchell, Training fMRI Classifiers to Detect Cognitive States across Multiple Human Subjects, IN NIPS03, vol. 16, 2003.

[4] J. V. Haxby, M. I. Gobbini, M. L. Furey, A. Ishai, J. L. Schouten, and P. Pietrini, Distributed and overlapping representations of faces and objects in ventral temporal cortex, Science, vol. 293, no. 5539, pp. 2425 2429, 2001.

[5] J.-D. Haynes and G. Rees, Predicting the orientation of invisible stimuli from activity in human primary visual cortex, Nat Neurosci, vol. 8, no. 5, pp. 686 691, 2005.

[6] C. Davatzikos, K. Ruparel, Y. Fan, D. G. Shen, M. Acharyya, J. W. Loughead, R. C. Gur, and D. D. Langleben, Classifying spatial patterns of brain activity with machine learning methods: Application to lie detection, NeuroImage, vol. 28, no. 3, pp. 663 668, 2005.

[7] T. M. Mitchell, R. Hutchinson, R. S. Niculescu, F. Pereira, X. Wand, M. Just, and S. Newman, Learning to decode cognitive states from brain images, Mach Learn, vol. 57, no. 1-2, pp. 145 175, 2004.

[8] S. M. Polyn, V. S. Natu, J. D. Cohen, and K. A. Norman, Category- specific cortical activity precedes retrieval during memory search, Science, vol. 310, no. 5756, pp. 1963 1966, 2005.

[9] D. J. Watts and S. H. Strogatz, Collective dynamics of small-world networks., Nature, vol. 393, no. 6684, pp. 440-2, Jun. 1998

[10] Y. He and A. Evans, Graph theoretical modeling of brain connectivity., Curr Opin NeuroI., vol. 23, no. 4, pp. 341 350, 2010.

[11] B. L. Schlaggar G. S.Wig and S. E. Petersen, Concepts and principles in the analysis of brain networks, Annals of the New York Academy of Sciences, vol. 1224, no. 1, pp. 126146, 2011.

[12] E. Bullmore and O. Sporns, Complex brain networks: graph theoretical analysis of structural and functional systems, Nature Reviews Neuroscience, vol. 10, pp. 186198, 2009.

[13] Y. He, Z. Chen, and A. Evans, Structural insights into aberrant topological patterns of large-scale cortical networks in alzheimers disease, The Journal of Neuroscience, vol. 28, no. 18, pp. 47564766, 2008.

[14] M. Ozay, I. Oztekin, U. Oztekin, and F. T. Y. Vural, Mesh learning for classifying cognitive processes, arXiv:1205.2382v2, 2013.

[15] O. Firat, M. Ozay, I. Onal, lke Oztekin, and F. T. Y. Vural, Functional mesh learning for pattern analysis of cognitive processes, in 12th IEEE International Conference on Cognitive Informatics and Cognitive Computing (ICCI*CC), 2013.

[16] I. Onal, M. Ozay, O. Firat, I. Oztekin, and F. T. Y. Vural, Analyzing the information distribution in the fmri measurements by estimating the degree of locality, in Proceedings of 35th Annual International Conference of the IEEE Engineering in Medicine and Biology Society (EMBS), 2013.

[17] C. Baldasano, M. C. Iordan, D. M. Beck, and L. Fei-Fei, Discovering voxel-level functional connectivity between cortical regions, in Machine Learning and In-

terpretation in NeuroImaging Workshop, NIPS, 2012.
[18] A. Zalesky, L. Cocchi, A. Fornito, M. M. Murray, and E. Bullmore, Connectivity differences in brain networks, NeuroImage, vol. 60, no. 2, pp. 1055 1062, 2012.
[19] T. Mitchell, S. V. Shinkareva, A. Carlson, K. Chang, V. L. Malave, R. A. Mason, and M. A. Just, Predicting human brain activity associated with the meanings of nouns, in Science, 2008, vol. 320, pp. 11911195.
[20] O. Sporns, The human connectome: a complex network, Annals of the New York Academy of Sciences, 2011, vol. 1224
[21] N. Tzourio-Mazoyer, B. Landeau, D. Papathanassiou, F. Crivelloand O. Etardand N. Delcroix, B. Mazoyer, and M. Joliot, Automated anatomical labeling of activations in spm using a macroscopic anatomical parcellation of the mni mri single-subject brain, NeuroImage, vol. 15, no. 1, pp. 273289, 2002.
[22] I. Onal, An Information Theoretic Representation of Brain Connectivity for Cognitive State Classification Using Functional Magnetic Resonance Imaging, METU Thesis, 2013.
[23] H. Akaike, Information theory and an extension of the maximum likelihood principle, in 2nd International Symposium on Information Theory, 1973, pp. 267 281.
[24] Rogers, B. P., Morgan, V. L., Newton, A. T., & Gore, J. C. (2007). Assessing functional connectivity in the human brain by fMRI. Magnetic resonance imaging, 25(10), 1347-1357.
[25] Zhou, D. (2011). Functional Connectivity Analysis of FMRI Time-Series Data (Doctoral dissertation, University of Pittsburgh).
[26] P. P. Vaidyanathan, The Theory of Linear Prediction. Morgan and Claypool Publishers, 2008.
[27] J. Sun, E. M. Bollt and D. ben-Avraham, Graph Compression - Save Information by Exploiting Redundancy, arXiv:0712.3312 2007
[28] N. S. Ketkar, L. B. Holder and D. J. Cook, Subdue: compression-based frequent pattern discovery in graph data, Proceedings of the 1st international workshop on open source data mining: frequent pattern mining implementations, pp. 71-76, 2005.
[29] M. Xia, J. Wang, and Y. He, Brainnet viewer: A network visualization tool for human brain connectomics. PLoS ONE, vol. 8, no. 7, 2013. [Online]. Available: http://www.nitrc.org/projects/bnv/